Gastroenterology 2017;153:1621–1633

Gavage of Fecal Samples From Patients With Colorectal Cancer Promotes Intestinal Carcinogenesis in Germ-Free and Conventional Mice

Sunny H. Wong,[1,*] **Liuyang Zhao**,[1,*] Xiang Zhang,[1] Geicho Nakatsu,[1] Juqiang Han,[1,2] Weiqi Xu,[1] Xue Xiao,[1] Thomas N. Y. Kwong,[1] Ho Tsoi,[1] William K. K. Wu,[3] Benhua Zeng,[4] Francis K. L. Chan,[1] Joseph J. Y. Sung,[1] Hong Wei,[4] and Jun Yu[1]

[1]Institute of Digestive Disease, Department of Medicine and Therapeutics, State Key Laboratory of Digestive Disease, Li Ka Shing Institute of Health Sciences and CUHK-Shenzhen Research Institute, The Chinese University of Hong Kong, Hong Kong, Hong Kong; [2]Institute of Liver Disease, Beijing Military General Hospital, Beijing, China; [3]Department of Anaesthesia and Intensive Care, The Chinese University of Hong Kong, Hong Kong, Hong Kong; and [4]Department of Laboratory Animal Science, College of Basic Medical Sciences, Third Military Medical University, Chongqing, China

See editorial on page 1475.

BACKGROUND & AIMS: Altered gut microbiota is implicated in development of colorectal cancer (CRC). Some intestinal bacteria have been reported to potentiate intestinal carcinogenesis by producing genotoxins, altering the immune response and intestinal microenvironment, and activating oncogenic signaling pathways. We investigated whether stool from patients with CRC could directly induce colorectal carcinogenesis in mice. **METHODS:** We obtained stored stool samples from participants in a metagenome study performed in Hong Kong. Conventional (male C57BL/6) mice were given azoxymethane to induce colon neoplasia after receiving a course of antibiotics in drinking water. Mice were gavaged twice weekly with stool from 5 patients with CRC or 5 healthy individuals (controls) for 5 weeks. Germ-free C57BL/6 mice were gavaged once with stool from 5 patients with CRC or 5 controls. We collected intestinal tissues from mice and performed histology, immunohistochemistry, expression microarray, quantitative polymerase chain reaction, immunoblot, and flow cytometry analyses. We performed 16S ribosomal RNA gene sequencing analysis of feces from mice. **RESULTS:** Significantly higher proportions of conventional mice fed with stool from individuals with CRC than control stool developed high-grade dysplasia ($P < .05$) and macroscopic polyps ($P < .01$). We observed a higher proportion of proliferating (Ki-67-positive) cells in colons of germ-free mice fed with stool from patients with CRC vs those fed with stool from controls ($P < .05$). Feces from germ-free and conventional mice fed with stool from patients with CRC vs controls contained different microbial compositions, with lower richness in mice fed with stool from patients with CRC. Intestines collected from conventional and germ-free mice fed with stool from patients with CRC had increased expression of cytokines that modulate inflammation, including C-X-C motif chemokine receptor 1, C-X-C motif chemokine receptor 2, interleukin 17A (IL17A), IL22, and IL23A. Intestines from conventional and germ-free mice fed with stool from patients with CRC contained higher proportions of T-helper 1 (Th1) cells (2.25% vs 0.44%) and Th17 cells (2.08% vs 0.31%) ($P < .05$ for each) than mice fed with stool from controls. Real-time polymerase chain reaction arrays revealed up-regulation of genes involved in cell proliferation, stemness, apoptosis, angiogenesis, invasiveness, and metastasis in mice fed with stool from patients with CRC. **CONCLUSIONS:** We fed stool samples from patients with CRC and heathy individuals to germ-free mice and conventional mice with azoxymethane. We found stool from patients with CRC to increase the numbers of polyps, levels of intestinal dysplasia and proliferation, markers of inflammation, and proportions of Th1 and Th17 cells in colon, compared with stool from individuals without CRC. This study provides evidence that the fecal microbiota from patients with CRC can promote tumorigenesis in germ-free mice and mice given a carcinogen.

Keywords: Colon Cancer; Stool Transplantation; Carcinogenesis; Germ-Free.

Emerging evidence suggests that the gut microbiota contributes to the carcinogenesis of colorectal cancer (CRC), along with genetic and other environmental factors. Early studies showed a reduction of tumor in the intestines of animals raised in a germ-free environment, in both genetically induced[1] and carcinogen-induced CRC rodent models.[2] The intestinal mucosa is a complex and dynamic interface between the host and the microbiota. Further studies have found that some bacteria, including *Escherichia coli*, *Bacteroides fragilis*, *Fusobacterium nucleatum*, and *Peptostreptococcus anaerobius*, may potentiate

***Authors share co-first authorship.**

Abbreviations used in this paper: **AOM, azoxymethane; CD, cluster of differentiation; CRC, colorectal cancer; CXCR, chemokine (C-X-R motif) receptor; DSS, dextran sulfate sodium; FITC, fluorescein isothiocyanate; HC, healthy control; IL, interleukin; IFN-γ, interferon gamma; NC, no stool gavage group; OTU, operational taxonomic unit; PBS, phosphate-buffered saline; PCNA, proliferating cell nuclear antigen; PCR, polymerase chain reaction; PE, phycoerythrin; PERMANOVA, permutational multivariate analysis of variance; rRNA, ribosomal RNA; RT-PCR, reverse transcription PCR; sobs, observed community richness.**

Most current article

0016-5085
https://doi.org/10.1053/j.gastro.2017.08.022

EDITOR'S NOTES

BACKGROUND AND CONTEXT

Colorectal cancer is associated with an altered gut microbiota. However, there are little data on the functional role of intestinal bacteria in carcinogenesis.

NEW FINDINGS

The researchers show that gavage of stools from colorectal cancer patients can promote intestinal carcinogenesis in mice in germ-free and carcinogen models.

LIMITATIONS

This study has not evaluated the effects of individual bacteria or their interactions.

IMPACT

The study provides evidence for the pro-tumorigenic role of the colorectal cancer microbiota.

intestinal carcinogenesis by producing genotoxin,[3,4] triggering Th17 immune response,[5] modulating the tumor microenvironment[6] and activating toll-like receptor and beta-catenin signaling in various murine models.[7,8]

Consistent with these findings, we and other groups have identified microbial changes and symbiotic networks across stages of colorectal carcinogenesis.[9–11] In a case-control study comparing the fecal microbiota of 74 patients with CRC and 54 controls, we have identified several novel bacteria and validated microbial markers potentially translatable into biomarkers for early cancer detection.[12] Our further work using paired mucosal samples revealed a disrupted bacterial ecology occurring early at the stage of adenoma during colorectal carcinogenesis.[11]

To investigate the effects and molecular basis of the microbial consortia on colorectal carcinogenesis, we gavaged mice with stool from human patients with CRC and healthy controls, and studied the phenotypic, pathologic, and molecular changes in the recipients. Using germ-free and carcinogen-induced conventional mouse models, we demonstrate that the CRC microbiota activates inflammatory and oncogenic pathways and promotes intestinal tumorigenesis.

Methods

Experimental Mice

The conventional male C57BL/6 mice were bred in the Laboratory Animal Services Centre at the Prince of Wales Hospital, the Chinese University of Hong Kong. In the mouse model of azoxymethane (AOM)-induced colon neoplasia, we gave antibiotics to adult mice (6 weeks of age) through drinking water containing 0.2 g/L ampicillin, neomycin, and metronidazole, and 0.1 g/L vancomycin daily for 2 weeks. After the last dose of antibiotics, the mice were injected with 1 dose of 10 mg/kg AOM intraperitoneally. After 1 week, the mice were divided into 3 groups each of 10 to 12 mice, and were gavaged twice weekly with stool from patients with CRC (CRC-A), healthy controls (HC-A), or phosphate-buffered saline (PBS) (NC-A) for 5 weeks. The controls were sibling littermates. The mice were killed 1 week after the last gavage.

The germ-free C57BL/6 mice were bred at the Department of Laboratory Animal Science at the Third Military Medical University in Chongqing, China. Adult mice (8 weeks of age) were divided into 2 groups each of 15 mice (8 male and 7 female) and were fed with stool from patients with CRC (CRC-G) or healthy controls (HC-G). The controls were sibling littermates. The oral gavage of stool samples was performed once (at week 0) for the germ-free mice. Five mice from each group were randomly selected and killed at week 8, week 20, or week 32 following the gavage.

To prepare the stool for gavage, 5 samples from patients with CRC and 5 samples from healthy individuals were selected at random and mixed at equal weight. One gram of the mixed stool was then suspended in 5 mL PBS. An aliquot of 200 μL suspension was used for gavage into each mouse. Separate sets of stool samples were used for the germ-free and AOM mice.

Human Stool Samples Collection

We fed stool to the AOM and germ-free mice, using stored fecal samples collected from a Hong Kong Chinese cohort that had been previously sequenced for a metagenome-wide association study.[12] This included adult individuals undergoing colonoscopy at the Shaw Endoscopy Centre at the Prince of Wales Hospital, the Chinese University of Hong Kong. This cohort included individuals presenting with digestive symptoms, such as change of bowel habit, rectal bleeding, abdominal pain, or anemia, as well as asymptomatic individuals aged $\geq$50 undergoing screening colonoscopy. The exclusion criteria were as follows: (1) use of antibiotics within the past 3 months; (2) on a vegetarian diet; (3) had an invasive medical intervention within the past 3 months; and (4) had a history of cancer or inflammatory disease of the intestine. Subjects were asked to collect stool samples in standardized containers at home and store the samples in their home freezer immediately. Frozen samples were delivered to the laboratory in insulating polystyrene foam containers and stored at -80°C immediately until use. All subjects had given written informed consent. The clinical study protocol was approved by the Clinical Research Ethics Committee of the Chinese University of Hong Kong.

Necropsy and Tissue Collection

At the end of the experiments, mice were anesthetized with sodium pentobarbital intraperitoneally (60 mg/kg) and the colon was excised longitudinally along the mesenteric margin. The colon was divided into 2 equal portions (proximal and distal), and the tissue samples were snap frozen in liquid nitrogen and kept at -80°C until analyzed. For the formalin-fixed samples, two 5-mm tissues were taken from the proximal and distal colorectum separately, and paraffin sectioning was done for every segment fixed.

Histological Evaluation

The proximal and distal segments of the colon were submitted for histological processing. All slides were stained with hematoxylin and eosin. Inflammation was assessed by infiltration of inflammatory cells into the epithelium, whereas dysplasia was defined by presence of hyperchromasia, nuclear pleomorphism, increased nuclear-to-cytoplasmic ratios, and atypical mitotic figures. The histology score consisted of a composite scale that indicated the overall degree of inflammation and

dysplasia (0 = absence of significant inflammation or dysplasia, 1 = mild inflammation without significant dysplasia, 2 = moderate inflammation with no or mild dysplasia, 3 = severe inflammation with at most moderate dysplasia, 4 = severe inflammation with severe dysplasia). The final composite score was calculated by the sum of 2 scores: 1 from the proximal segment and 1 from the distal segment, respectively.

Immunohistochemistry Staining

Paraffin-embedded tissues were used for analyzing the expression of Ki-67 and proliferating cell nuclear antigen (PCNA). After deparaffinization, the slides were heated in an autoclave with sodium citrate for antigen repairing, followed by 1% hydrogen peroxide to abolish endogenous peroxidase activity, and 2% goat serum for blocking. Slides were then incubated with primary antibody (1:100) at 4°C overnight. Signals were developed with VECTASTAIN Elite ABC kit (Vector Laboratories, Burlingame, CA) and DAB (Dako, Agilent Technologies, Santa Clara, CA). The proportion of Ki-67– or PCNA-positive cells was determined by counting immunostain-positive cells, as a percentage to the total number of nuclei in the field. At least 1000 cells were counted in 5 random microscopic fields.

Microbial DNA Extraction and Sequencing

Total genomic DNA from 100 mg of stool (stool from CRC-G and HC-G mice at 8 weeks and 32 weeks after stool gavage, and stool from CRC-A and HC-A at 6 weeks after start of stool gavage) was extracted by QIAamp DNA Stool Mini Kit (QIAGEN, Valencia, CA) and quantified by Agilent 2100 Bioanalyzer. Polymerase chain reaction (PCR) amplification of V4 regions of bacterial 16S ribosomal RNA (rRNA) genes for paired end sequencing (2 × 250 bps) on the Illumina MiSeq platform (Illumina, Inc, San Diego, CA) was performed using universal primer sequences (515F, 5′-GTGCCAGCMGCCGCGGTAA-3′; 806R, 5′-GGACTACHVGGGTWTCTAAT-3′). PCR products were quantified by Quant-iT PicoGreen dsDNA Assay Kit (Life Technologies, Carlsbad, CA), and amplicon libraries were prepared using SequelPrep Plate Normalization kit (Life Technologies) according to the manufacturer's instructions.

16S rRNA Gene Sequence Analysis

Raw de-multiplexed FASTQ files were preprocessed in Mothur.[13] Contigs were created using Needleman-Wunsch alignment algorithm with default parameters,[14] and aligned against the SILVA database (version 128) using the NAST algorithm.[15,16] We removed any contigs with homopolymers of greater than 8 nucleotides and retained all that mapped within the SILVA coordinates. Any sequence pairs with mismatch difference of ≤2 were preclustered to reduce amplicon sequencing noises. Chimeric sequences were culled using de novo UChime.[17] Post–quality controlled sequences were classified using the naïve Bayesian classifier (n = 1000; average pseudo-bootstrapped confidence scores ≥80%) trained on 16S rRNA gene sequence collection from the Ribosomal Database Project (version 16), which was supplied with standard species-level taxonomic ranks, 119 mitochondrial 16S rRNA gene sequences of Rickettsiales, and 4 Eukarya 18S rRNA gene sequences.[18] We discarded any sequences of eukaryotic, archaic, mitochondrial, chloroplastic, or unknown origins before binning them into operational taxonomic units (OTUs) at 97% identity threshold using the OptiClust algorithm.[19] The lowest taxonomic annotation for an OTU was defined as having a consensus assignment score of ≥80. Sequence count table was rarefied to the smallest number of reads per sample (ie, 12,486 reads) to reduce the effects of variable sequencing depths on downstream analyses. Differential abundance analysis was performed using the all-against-all detection algorithm of LEfSe program.[20] We filtered differentially abundant OTUs by false discovery rate–adjusted significance of ≤ 0.05 from linear discriminant analysis. Average robust fold change for each OTU was computed using the *fcros* package in the R Project for Statistical Computing, by pairwise sample comparison with the default quartile feature exclusion criteria based on fold change rank-order statistics.[21]

RNA Extraction and Quantitative Reverse-Transcription PCR (RT-PCR)

Total RNA was isolated from the colonic mucosae using the TRIzol Reagent (Invitrogen, Carlsbad, CA). Complementary DNA was synthesized from total RNA using Transcriptor Reverse Transcriptase (Roche, Basel, Switzerland). Real-time PCR was performed using SYBR Green master mix in the Light Cycler 480 Real-Time PCR system (Roche). The relative RNA expression was normalized to that of beta-actin or glyceraldehyde 3-phosphate dehydrogenase as denominators.

RT2 Profiler PCR Array Gene Expression

Total RNA was isolated from the colonic mucosae using the TRIzol Reagent (Invitrogen). RNA quality was determined using a spectrophotometer and was reverse transcribed using a complementary DNA conversion kit. The complementary DNA was used on the real-time RT^2 Profiler PCR Array Mouse Inflammatory Response and Autoimmunity (catalog no. PAMM-077Z; QIAGEN) or RT^2 Profiler PCR Array Mouse Cancer PathwayFinder (Catalog no. PAMM-077Z; QIAGEN) in combination with SYBR Green qPCR Mastermix (Roche). Cycle threshold values were exported to a table for analysis, which were normalized based on a full panel of reference genes. The fold changes were calculated using the delta-delta cycle threshold method. Genes with fold changes more than or less than 2 were considered to be of biological significance.

Fluorescence Activated Cell Sorting

Flow cytometry cell sorting was performed to study the immune cell type in the colonic mucosae, blood, and spleen of the germ-free mice. For the intestine, tissues were dissected and incubated in Hank's balanced salt solution with 0.1 mg/mL collagenase D (Roche) and 50 U/mL DNase I (Roche) for 30 minutes at 37°C. Cells were then resuspended in staining solution (PBS with 2% fetal calf serum) for flow cytometry. For the blood and spleen tissues, red blood cells were removed with ammonium-chloride-potassium lysis buffer. The cell suspension was filtered with a 70-μm cell strainer, washed with PBS, and resuspended in staining solution for flow cytometry.

Cells were treated with Fc receptor blocker rat anti-mouse CD16/CD32 (BD Pharmingen, San Jose, CA) for 30 minutes. Cells were then stained with fluorochrome-conjugated monoclonal antibodies: fluorescein isothiocyanate (FITC) anti-mouse CD3ε (145–2C11), phycoerythrin (PE) anti-mouse natural killer (NK)-1.1 (PK136), PE anti-mouse CD4 (H129.19), PE/Cy5 anti-mouse CD8a (53–6.7), APC anti-mouse CD19 (6D5), FITC

anti-mouse CD11b (M1/70), PE anti-mouse F4/80 (BM8), APC anti-mouse Ly-6G (1A8), FITC anti-mouse interferon (IFN)-γ (XMG1.2), PE anti-mouse interleukin (IL)17A (TC11–18H10.1). All antibodies and relative isotype controls were purchased from BioLegend. For intracellular IFN-γ and IL17 staining, cells were treated with 50 ng/mL phorbol myristate acetate (Sigma-Aldrich, St Louis, MO), 500 ng/mL ionomycin (Sigma-Aldrich), and 2 M monensin (BioLegend, San Diego, CA) for 5 hours by Cytofix/Cytoperm fixation/permeabilization kit (BD Biosciences, San Joe, CA). Samples were analyzed by BD FACS Canto and subsequent analysis was performed with FlowJo software (Treestar, Inc, San Carlos, CA). All assays were performed in triplicate.

Western Blot

Protein lysates from cell lines were prepared using protease inhibitor cocktail–containing (Roche) lysis buffer. Protein concentration was determined by the Bradford method (Bio-Rad Laboratories, Hercules, CA). Antibody-antigen complexes were detected using the ECL Plus Western Blotting Detection Reagents (GE Healthcare, Piscataway, NJ). Primary antibodies used were mouse anti-Aurora A (Abcam, Cambridge, UK), rabbit anti-Cdc20 (Cell Signaling Technology, Danvers, MA), and mouse anti-β-actin (Santa Cruz Biotechnology, Dallas, TX).

Statistical Analysis

All measurements were shown as mean ± standard deviation. Mann-Whitney *U* or Wilcoxon's rank-sum test was used to test for differences in numerical variables, and Fisher's exact test was used to evaluate the proportional difference in categorical variables between groups. Permutational multivariate analysis of variance (PERMANOVA) test was used to assess the difference in microbial compositions due to treatment or disease group factors. We used observed community richness (sobs) and Chao1 community richness (Chao1) indexes for comparison of bacterial OTU richness, and Fisher's alpha diversity and Shannon-Weaver's diversity indexes for comparison of bacterial OTU diversity. All statistical tests were performed with the R Project for Statistical Computing and GraphPad Prism 7.0 (GraphPad, La Jolla, CA). A 2-tailed $P \leq .05$ was considered statistically significant.

Ethical Statement

All animal protocols were approved by the Animal Experimentation Ethics Committees of the Chinese University of Hong Kong and Third Military Medical University in China. The experiments were conducted in adherence to the Animal Research: Reporting of In Vivo Experiments (ARRIVE) guidelines. Human stool samples were collected according to protocol approved by the Joint Chinese University of Hong Kong–New Territories East Cluster Clinical Research Ethics Committee.

Results

CRC Stool Promotes Intestinal Tumorigenesis in an AOM Mouse Model

To investigate the effects of gut microbiota on intestinal tumorigenesis, we gavaged human stool to mice treated with a single injection of AOM, a commonly used experimental carcinogen (Figure 1*A*). After microbiota depletion with antibiotics and intraperitoneal injection of AOM, mice randomly received stool from patients with CRC (CRC-A group, n = 11) and healthy controls (HC-A group, n = 12), respectively. Another group of mice received no stool gavage (NC-A group, n = 10). All the mice were housed and harvested at end of week 9, and their colons were examined.

Macroscopic examination showed that 7 mice had colonic polyps in the CRC-A group (7/11 = 63.6%), significantly more than that of the 2 other groups ($P < .01$; Figure 1*B*), with 2 mice in the HC-A group (2/12 = 16.7%) and 1 mouse in the NC-A group (1/10 = 10%; Supplementary Table 1). The number of polyps in the CRC-A group (1.45 per mouse) was significantly higher than that of the 2 other groups (average 0.27 per mouse, $P < .01$; Supplementary Table 1). All polyps were located in the distal colon and were similar in size between groups ($P > .05$; Supplementary Table 1). Three mice harbored high-grade dysplasia in the colon in the CRC-A group (3/11 = 27.3%; Figure 1*C* and *D*), compared with none in the HC-A or NC-A groups ($P < .05$; Supplementary Table 1; Figure 1*C* and *D*). Nine mice were observed to have histological inflammation in the CRC-A group (9/11 = 81.8%), significantly more than the 2 other groups (8/22 = 36.4%, $P < .05$; Supplementary Table 1). Overall, there was a significantly higher composite histology score in the CRC-A group (4.45 ± 1.81) than the 2 control groups (average score 2.82 ± 1.47, $P < .05$; Figure 1*E*; Supplementary Table 1), indicating more mucosal dysplasia and inflammation in mice that received stool from patients with CRC.

CRC Stool Increases Colonocyte Proliferation in a Germ-Free Mouse Model

To study the effects of the CRC stool independent of the preexisting microbial milieu, we gavaged stool from patients with CRC and healthy controls to germ-free mice (CRC-G and HC-G group, n = 15 each). Another group of mice received PBS with no stool gavage (NC-G group, n = 15). Mice were harvested and examined at different time points of weeks 8, 20, and 32 (Figure 2*A*).

Germ-free mice receiving stool gavage in the CRC-G and HC-G groups showed a more well-developed mucosal structure than the germ-free mice receiving no gavage in the NC-G group. We observed no visible histological differences between mice in the CRC-G or HC-G groups. Nevertheless, we observed increased epithelial cell proliferation in the colons of the CRC-G group compared with the HC-G group at 20 weeks (50.2% vs 47.2%, $P < .05$) and 32 weeks (48.6% vs 40.0%, $P < .05$) after stool gavage, as indicated by a higher proportion of Ki-67-positive cells (Figure 2*B*). Although the difference in Ki-67 protein expression did not reach statistical significance ($P > .05$, Figure 2*C*), we observed increased PCNA immunostaining ($P < .01$, Figure 2*D*) and protein expression in Western blot ($P < .05$, Figure 2*E*), as well as a higher active β-catenin protein expression in Western blot ($P < .05$, Figure 2*F*) in the CRC-G

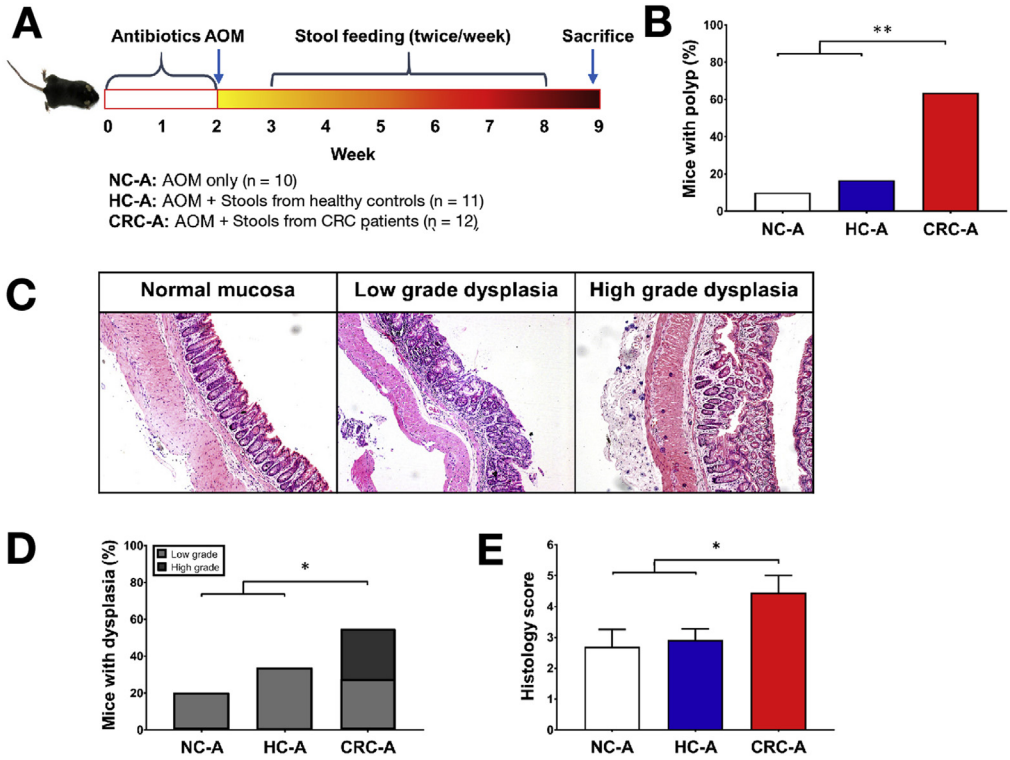

Figure 1. Effects of CRC and control stool on intestinal tumorigenesis in the AOM mouse model. (*A*) Design of stool gavage experiment to AOM-treated mice (NC-A group n = 10, HC-A group n = 11, CRC-A group n = 12). (*B*) Number of mice with macroscopic polyps. Proportions of mice with polyps were compared using the Fisher's exact test. (*C*) Histological slides showing normal and dysplastic mucosae in the experiment. (*D*) Number of mice harboring low- and high-grade dysplasia. Proportions of mice showing high-grade dysplasia were compared using the Fisher's exact test. (*E*) Histology score indicating degree of inflammation and dysplasia in AOM mice receiving CRC and control stool. Composite scores were compared using the Mann-Whitney *U* test. *$P < .05$, **$P < .01$.

group at 32 weeks after stool gavage. Taken together, these data suggest that the CRC microbiota promoted colonic epithelial cell proliferation in germ-free mice especially after a prolonged period of colonization.

Distinct Gut Microbiota Development in Mice Receiving Stool from CRC and Healthy Subjects

We performed 16S rRNA gene sequencing on stool collected from mice in both AOM and germ-free models, after feeding stool from 5 patients with CRC and 5 healthy controls to mice in each model. Clinical characteristics of the donors are described in Supplementary Tables 2 and 3. Reanalyzing sequence data from our previous metagenome-wide association study,[12] PERMANOVA showed that the case-control status was a significant factor affecting the microbial profile (AOM group, $P < .05$; germ-free group, $P < .05$). The relative abundance of selected bacteria, including *F nucleatum*, *P anaerobius* and some other putative species are shown in Supplementary Table 4. Principal coordinates analysis showed separate clusters of donor fecal microbiota for CRC and control statuses (Supplementary Figure 1).

In the AOM model, CRC-A and HC-A mice developed different gut microbiota after stool gavage. PERMANOVA showed donor stool status as a significant factor in driving the difference in microbial composition of the recipient mice ($P < .001$). Nonmetric multidimensional scaling analysis demonstrated clear separation of bacterial OTU composition (PERMANOVA, $P < .001$; Figure 3*A*). We observed a significantly lower bacterial richness in the CRC-A group (sobs, $P < .01$; Chao1, $P < .001$; Figure 3*B*). Comparisons of bacterial diversity are detailed in Supplementary Table 5. Differential relative abundance analysis of fold change identified 24 significant OTUs separating the 2 treatment groups (Figure 3*C*).

In the germ-free model, the donor stool status was also a significant factor contributing to differences in microbiota composition, at 8 weeks (PERMANOVA, $P < .001$) and 32 weeks (PERMANOVA, $P < .001$) after stool gavage. Nonmetric multidimensional scaling analysis showed segregation of gavage groups at different time points (Figure 4*A*). We observed lower Shannon-Weaver's diversity indexes in the CRC-G group, compared with the HC-G group at the 8-week time point (Wilcoxon's rank-sum test; $P < .001$; Figure 4*B*). Observed community richness, but not Chao1, was significantly different at 8 weeks between HC-G and CRC-G groups (Wilcoxon's rank-sum test; sobs, $P < .01$; Chao1, $P > .05$; Supplementary Table 5). The microbiota continued to evolve beyond 8 weeks after stool gavage, resulting in a significant shrinkage in OTU richness at 32 weeks (HC-G group, $P < .01$; CRC-G group, $P < .01$; Figure 4*B*). Despite overall compositional change, some CRC-associated signature remained evident as the microbial

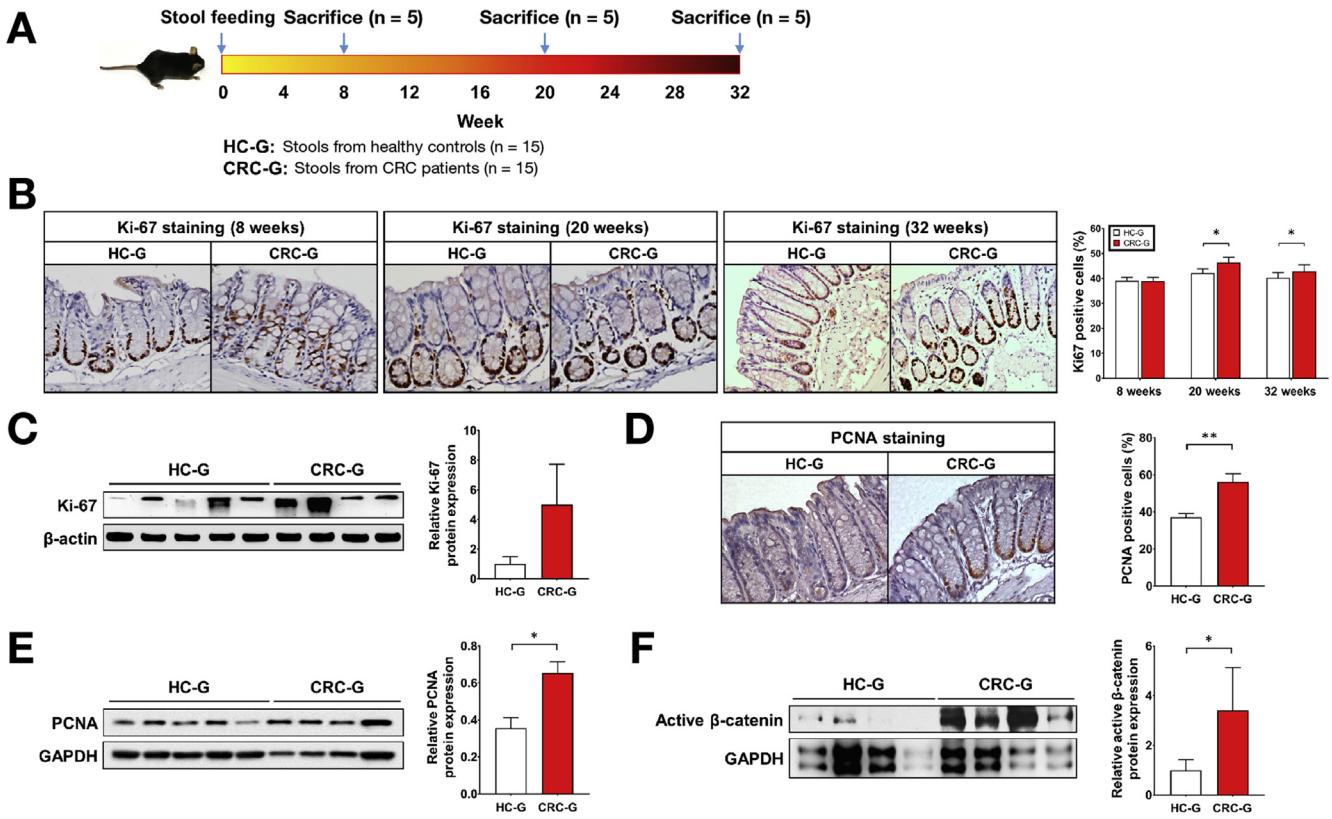

Figure 2. Effects of CRC and control stool on cell proliferation in the germ-free mouse model. (*A*) Design of stool gavage experiment to germ-free mice (HC-G group n = 15, CRC-G group n = 15). (*B*) Immunohistochemistry showing Ki-67–positive cells in the colon of germ-free mice at 8 weeks, 20 weeks, and 32 weeks after stool gavage, and the proportion of Ki-67–positive cells in the colon of germ-free mice. Ratios were compared using the Mann-Whitney *U* test. (*C*) Western blot showing relative protein expression of Ki-67 in the colon of germ-free mice at 32 weeks after stool gavage. Relative expressions were compared using the Mann-Whitney *U* test. (*D*) Immunohistochemistry showing PCNA-positive cells in the colon of germ-free mice at 32 weeks after stool gavage. Ratios were compared using the Mann-Whitney *U* test. (*E*) Western blot showing relative protein expression of PCNA in the colon of germ-free mice at 32 weeks after stool gavage. Relative expressions were compared using the Mann-Whitney *U* test. (*F*) Western blot showing relative protein expression of active β-catenin in the colon of germ-free mice at 32 weeks after stool gavage. Ratios were compared using the Mann-Whitney *U* test. *$P < .05$; **$P < .01$

composition in the CRC-G group was significantly different from the HC-G group at 32 weeks (PERMANOVA, $P < .01$). Differential multiclass fold change analysis revealed 64 OTUs that differentiated treatment time points across HC-G and CRC-G groups (Figure 4*C*). These included the enrichment of *B fragilis* OTU (LEfSe; OTU488, adjusted $P < .05$) in the CRC-G group at 32 weeks, and depletions of *Faecalibacterium prausnitzii* OTUs (LEfSe; OTU23, adjusted $P < .001$; OTU578, adjusted $P < .001$), *Clostridium* cluster OTUs (LEfSe; OTU116, adjusted $P < .001$; OTU150, adjusted $P < .001$), and numerous Lachnospiraceae OTUs (LEfSe; OTU161, adjusted $P < .001$; OTU190, adjusted $P < .001$; OTU295, adjusted $P < .001$; OTU170, adjusted $P < .001$; OTU334, adjusted $P < .001$; OTU434, adjusted $P < .05$) in the CRC-G group at 8 and 32 weeks after stool gavage.

CRC Stool Increases Expression of Proinflammatory Genes in AOM and Germ-free Mice

To gain insights into the molecular basis underlying the pro-tumorigenic effect of the stool from patients with CRC, we studied the gene expression profile of colonic cells at 8 weeks after gavage in the AOM model and at 20 weeks after gavage in the germ-free model. We used the Mouse Inflammatory Response and Autoimmunity PCR Array to profile the expression of 84 key genes involved in inflammatory response. The data showed up-regulation of 33 genes for more than twofold in both models, many of which encoding for cytokines and their receptors (Figure 5*A*, Supplementary Table 6). The gene ranks in both microarrays were highly correlated with each other (Spearman's *rho* = 0.52, $P < .001$). These included the genes *chemokine (C-X-C motif) receptors 1 (Cxcr1)* and *2 (Cxcr2)*, both overexpressed for more than 15-fold and encoded for 2 homologous receptors to induce neutrophil chemotaxis. The list also included the genes *interleukin 17a (Il17a)*, *Il22*, and *Il23a*, encoding for 3 cytokines secreted by Th17 lymphocytes, as well as *interferon gamma (Ifng)* encoding for the Th1 effector cytokine IFN-γ. The gene *toll-like receptor 5 (Tlr5)* was significantly down-regulated in both microarrays. Taken together, these genes corresponded to the immune system involving chemotaxis, antigen presentation, proinflammatory response, and the

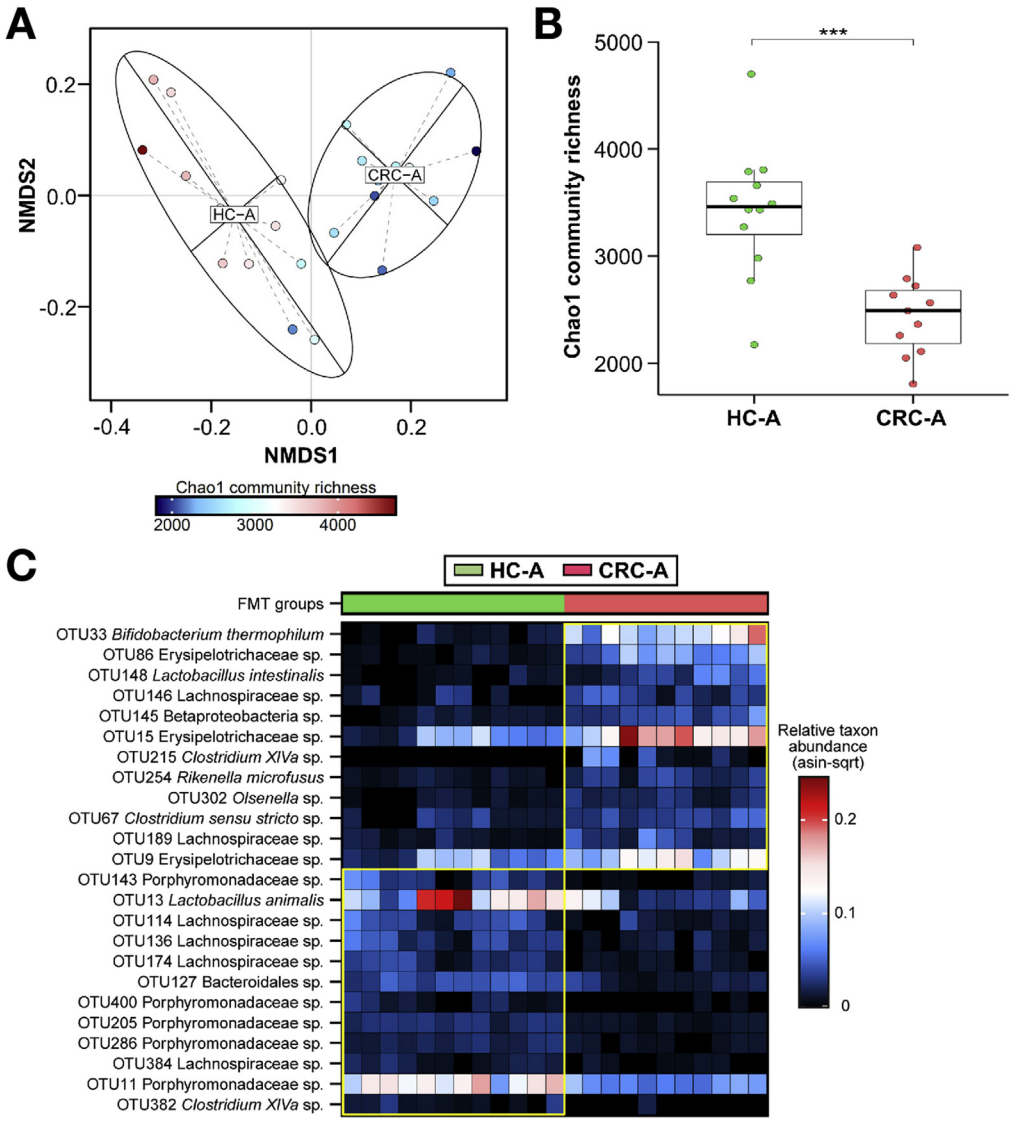

Figure 3. Gut microbiota in AOM mice after stool gavage. (*A*) Nonmetric multidimensional scaling (NMDS) ordination analysis of bacterial OTU community distance based on Bray-Curtis dissimilarity metrics of relative abundance profiles (HC-A, n = 12; CRC-A, n = 11). Data points are grouped by 95% confidence ellipses and color-coded by the magnitude of alpha index. (*B*) Comparison of Chao1 community richness between HC-A and CRC-A groups. The richness indexes were compared using the Wilcoxon rank-sum test. (*C*) Relative abundance heat-map of differentially enriched bacterial OTUs in AOM mice receiving CRC and healthy control stool. OTUs with false discovery rate $\leq$ .05, and average robust fold enrichment of $\geq$ 4 coupled with fold depletion of $\leq$ 1 are reported. ***$P < .001$.

Th17 pathway (Figure 5*B*). Quantitative RT-PCRs using specific primer-probes were performed on genes identified in the microarray study, confirming the changes in expression of *Il17a, Il22, Il23a*, and *chemokine (C-X-C motif) ligand 2* (Figure 5*C*).

CRC Stool Increases Immune Cells Infiltration in AOM and Germ-Free Mice

Immune cells and their effectors are key components that promote neoplastic progression. As Th1- and Th17-related cytokines were up-regulated by CRC microbiota in germ-free mice, we characterized the Th1 and Th17 immune cells from the intestinal tissues of germ-free mice receiving stool gavage from the patients with CRC or healthy controls. Th1 ($CD4^+$ IFN-γ^+) and Th17 ($CD4^+$ IL-17^+) immune cells were significantly increased in intestines of germ-free mice in the CRC-G group compared to mice in the HC-G group (Th1 cells: 2.25% vs 0.44%, $P < .05$; Th17 cells: 2.08% vs 0.31%, $P < .05$, Figure 5*D*). In addition, we evaluated the systemic immune response by analyzing immune cell populations in the spleen and peripheral blood of mice receiving stool from the CRC-G and HC-G groups using flow cytometry. We did not find any difference for the abundance of NK cells ($NK1.1^+$ $CD3^-$), NKT cells ($NK1.1^+$ $CD3^+$), $CD4^+$ T cells ($CD4^+$ $CD3^+$), $CD8^+$ T cells ($CD8^+$ $CD3^+$), neutrophils ($CD11b^+$ $Ly6G^+$), macrophages ($CD11b^+$ $F4/80^+$), B cells ($CD19^+$ $CD3e^-$), dendritic cells ($CD11c^+$ $CD3e^-$), Th1 ($CD4^+$ IFN-γ^+), and Th17 ($CD4^+$ IL-17^+) in the peripheral blood and spleen of CRC-G and HC-G groups at 8 weeks after stool gavage.

CRC Stool Increases Expressions of Oncogenic Factors in AOM and Germ-Free Mice

Furthermore, we profiled the expression of genes involved in cancer pathways using the Mouse Cancer Pathway Finder PCR Array, using colonic cells at 8 weeks after gavage in the AOM model and at 20 weeks after gavage in the germ-free model. This microarray consists of

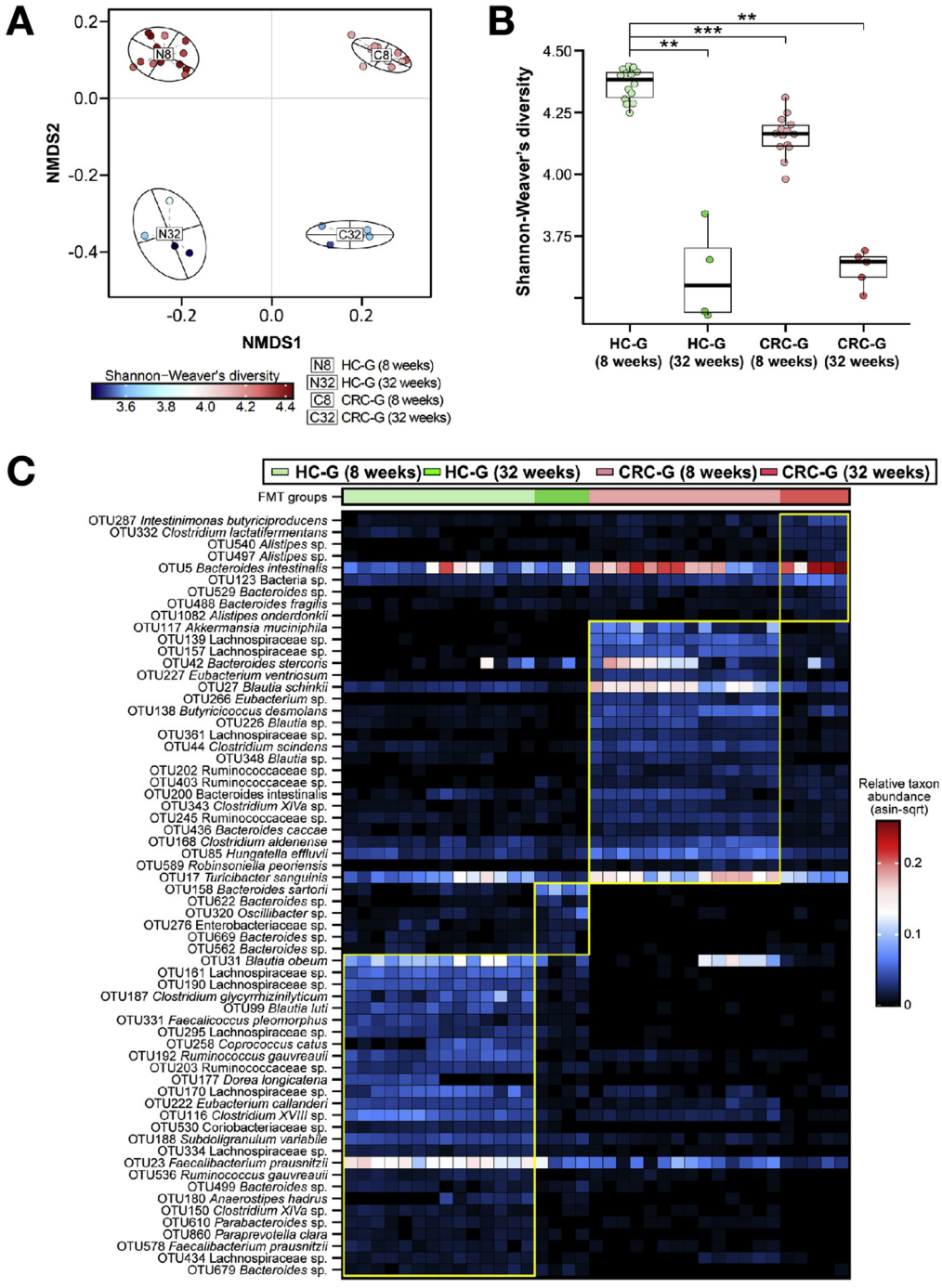

Figure 4. Evolution of gut microbiota in germ-free mice after stool gavage. (*A*) Nonmetric multidimensional scaling (NMDS) ordination analysis of bacterial OTU community distance based on Bray-Curtis dissimilarity metrics of relative abundance profiles (HC-G 8 weeks, n = 14; HC-G 32 weeks, n = 4; CRC-G 8 weeks, n = 14; CRC-G 32 weeks, n = 5). Data points are grouped by 95% confidence ellipses and color-coded by the magnitude of alpha index. (*B*) Comparison of Shannon-Weaver's diversity indexes between the HC-G and CRC-G groups at 8 weeks and 32 weeks after stool gavage. The diversity indexes were compared using the Wilcoxon rank-sum test and controlled for false discovery rate. (*C*) Relative abundance profiles of differentially enriched bacterial OTUs in germ-free mice receiving CRC and healthy stool, at 8 weeks and 32 weeks after stool gavage. OTUs that have false discovery rate $\leq .05$, as well as average robust fold increase of ≥ 4 coupled with fold decrease of ≤ 1 are reported. **Adjusted $P < .01$, ***adjusted $P < .001$.

84 genes representing major biological pathways involved in tumorigenesis. Results showed up-regulation of 37 genes for more than twofold in both models (Figure 6*A*, Supplementary Table 7). These genes were involved in oncogenic pathways including cell proliferation, stemness, apoptosis, angiogenesis, tumor invasiveness, and metastasis (Figure 6*B*). Up-regulation of the several genes including *marker of proliferation Ki-67 (Mki67), minichromosome maintenance complex component 2 (Mcm2), aurora kinase A (Aurka), cell-division cycle 20 (Cdc20),* and *B Lymphoma Mo-MLV Insertion Region 1 Homolog (Bmi1)* were validated by quantitative RT-PCR using specific primer-probes (Figure 6*C*).

Discussion

Despite the increasing evidence to implicate the gut microbiota in CRC, the collective role of the microbial consortia on colorectal carcinogenesis is underinvestigated. This study provides evidence for the direct pro-tumorigenic effect of the CRC microbiota, as a whole, in conventional and germ-free mouse models.

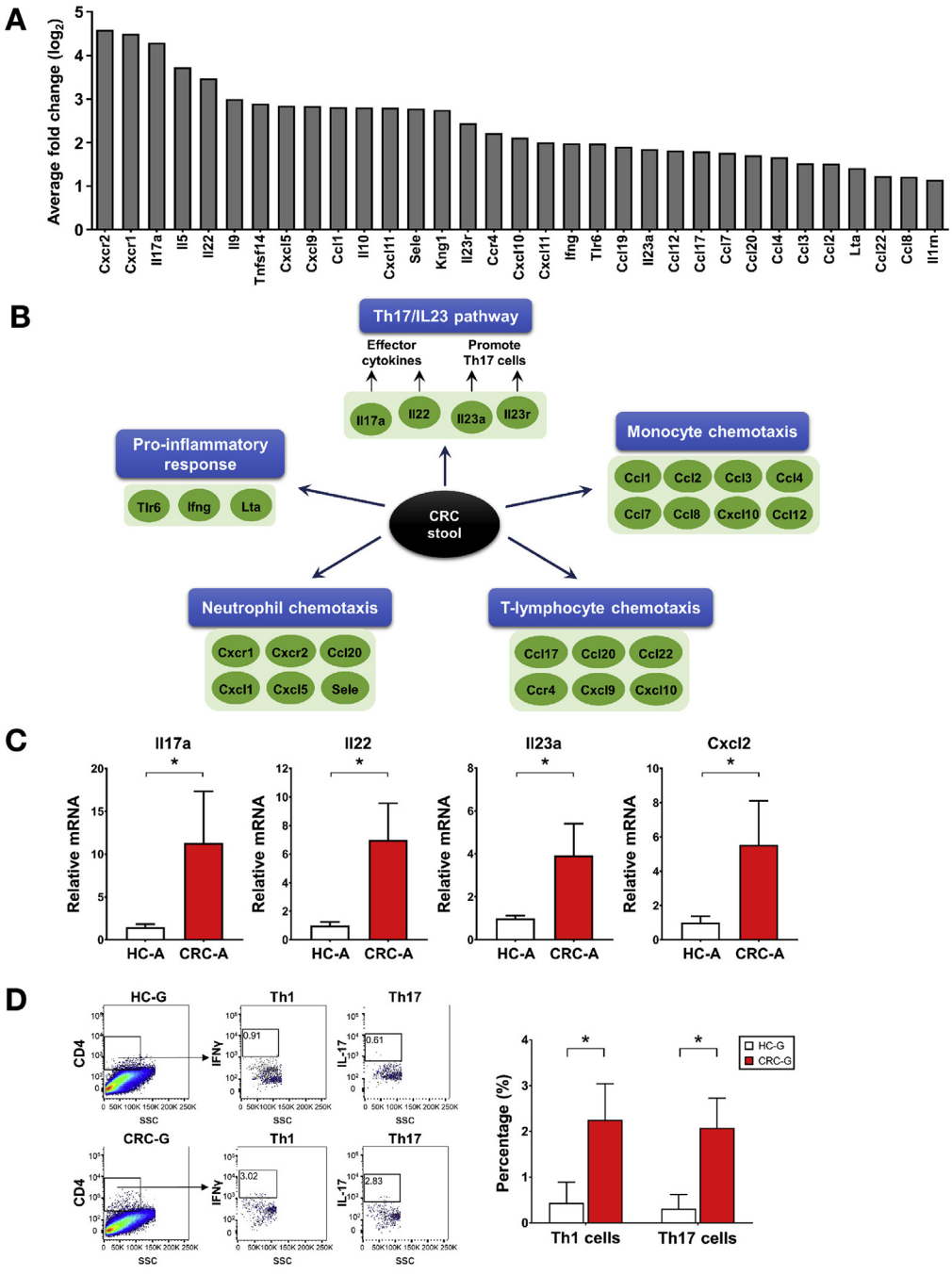

Figure 5. Effects of CRC stool on inflammatory factors. (*A*) Significant up-regulation in the expression of 33 transcripts by the Mouse Inflammatory Response and Autoimmunity PCR Array, after gavage of CRC stool to both AOM and germ-free mouse models. (*B*) A systematic diagram showing major inflammatory pathways implicated by up-regulated genes identified by the PCR array. (*C*) Quantitative RT-PCR validation was performed to confirm changes in expression of genes including *Il17a*, *Il22*, *Il23a*, and chemokine (C-X-R motif) ligand *(Cxcl2)*. Expression levels were compared using the Mann-Whitney *U* test. (*D*) Flow cytometry analysis showing increased Th1 and Th17 cell infiltration in the colon of a germ-free mouse receiving CRC stool gavage. Bar charts showing proportion of Th1 and Th17 cells in the colons of the germ-free mice receiving CRC stool gavage. Percentages of Th1 and Th17 cells were compared using the Mann-Whitney *U* test. $^{*}P < .05$, $^{**}P < .01$.

The gut microbiota has co-evolved with humans to form a symbiotic relationship that is important for life. Although these microorganisms can furnish the host with important nutrients and help mature the immune system, this mutualism comes at the expense of an increased incidence of some diseases, including cancers. Studies in germ-free animals have shown pro-tumorigenic effects of the microbiota in spontaneous, genetically induced and carcinogen-induced CRC.[1,2] Several individual bacteria have been pinpointed[3–7]; nevertheless, it is unknown whether the pro-tumorigenic effects are pervasive to commensal species across different bacterial phyla, or whether they are specific to a defined set of cancer microbiota. With a higher rate of high-grade dysplasia among mice fed with stool from patients with CRC than those from healthy controls, our study suggests that a defined set of microbiota may be important for CRC carcinogenesis. The composition of the microbiota is important in producing the phenotype, given the distinctive microbial patterns in stool from patients with CRC and controls. The absence of significant dysplasia in the control group suggests that human commensals may not be pro-tumorigenic, at least in the current AOM model, although we cannot differentiate whether these stools are mechanistically neutral or protective against colorectal neoplasia.

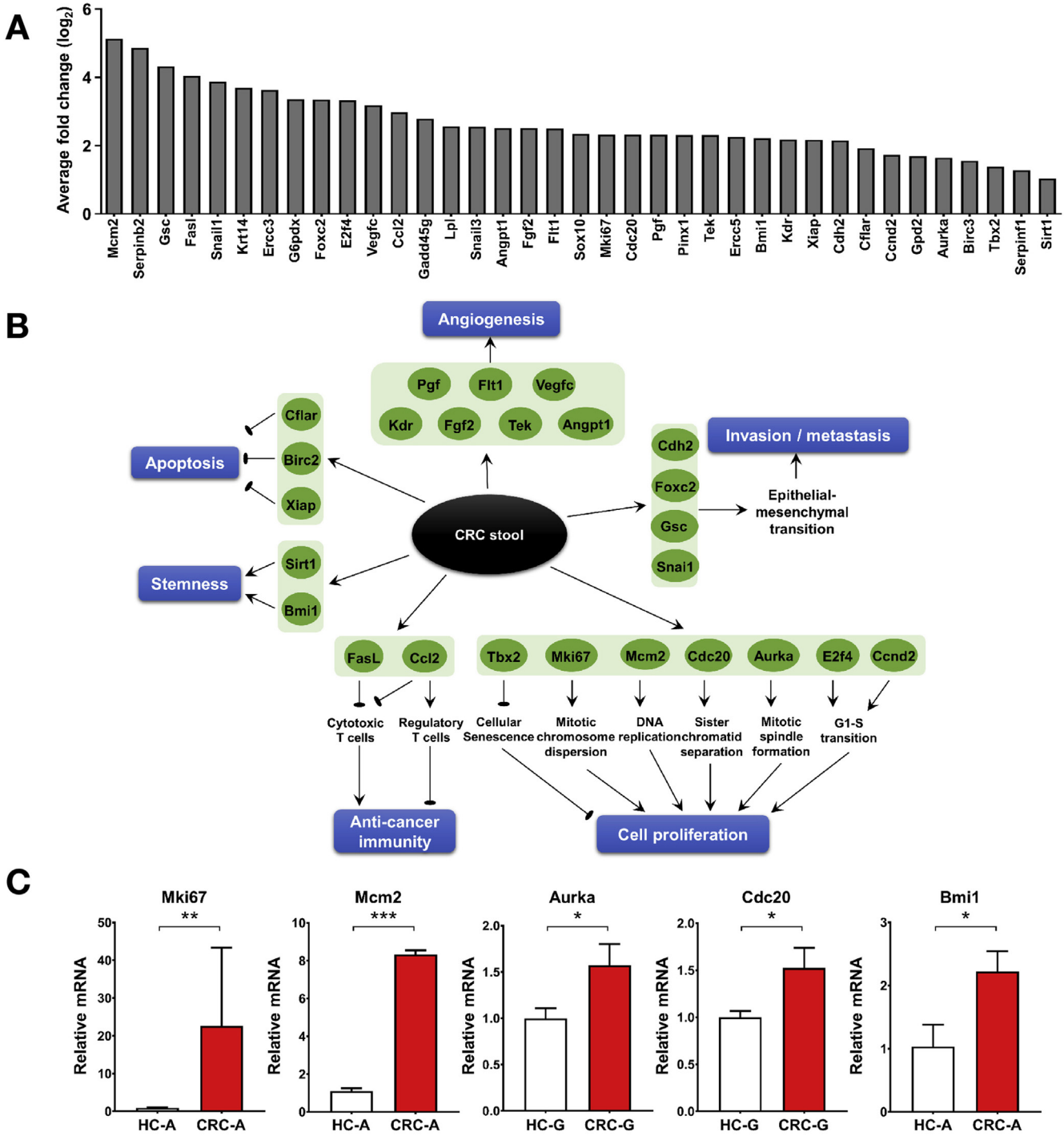

Figure 6. Effects of CRC stool on oncogenic factors. (*A*) Significant up-regulation in the expression of 37 transcripts by the Mouse Cancer Pathway Finder PCR Array. (*B*) A systematic diagram showing major oncogenic pathways implicated by up-regulated genes identified by the PCR array. (*C*) Quantitative RT-PCR validation was performed to confirm changes in expression of genes, including *Mki67*, *Mcm2*, *Aurka*, *Cdc20*, and *Bmi1*. Expression levels were compared using the Mann-Whitney *U* test. (*D*) Western blot showing relative protein expression of aurora kinase A and Cdc20 in the colons of germ-free mice. $^{*}P < .05$, $^{**}P < .01$, $^{***}P < .001$

We fed human stool to AOM-treated mice to study the effect of gut microbiota on intestinal tumorigenesis. The pro-tumorigenic effect of the CRC microbiota was supported by the increased number of polyps as well as histological dysplasia and inflammation. This suggested that the stool content was an important factor in determining the phenotypes, in carcinogen-treated mice with a mature immune system developed under a conventional environment. This contrasts with germ-free mice that have a deficient immune system, including underdevelopment of

the gut-associated lymphoid tissues. We observed increased epithelial cell proliferation in germ-free mice receiving stool from patients with CRC. Although the absolute difference of 3% (50.2% vs 47.2%) in the proportion of Ki-67–positive cells at 20 weeks may look trivial, this small difference in growth fraction at a cross-sectional snapshot can translate into large cumulative differences. Assuming turnover of a colonic epithelial cell is 5 days, and the cell death rate remains unchanged, a 3% increase in cell proliferation will lead to a more than twofold increase in epithelial mass in 120 days; whereas the 8.6% difference in proliferative index at 32 weeks (48.6% vs 40.0%) will translate into a more than sevenfold increase in epithelial mass over the same period. Consistent with the immunohistochemistry results, we have observed increases in *Mki67* gene expression in the microarray and quantitative RT-PCR validation analyses. As such, this increase in proliferation index can be biologically relevant to the oncogenic initiation of a tumor.

Our study is also unique in having stool mixed from 5 patients with CRC, giving a polymicrobial cocktail of organisms that were fed to the mice. This is important to the mechanistic study of CRC microbiota. Previous studies have identified several bacteria that can promote carcinogenesis by different mechanisms, such as genotoxic *polyketide synthase* (*pks*)-harboring *Escherichia coli*, which can cause direct DNA damage[4]; *F nucleatum* which can produce FadA adhesin to modulate E-cadherin/beta-catenin signaling,[7] and *P. anaerobius* which can induce cholesterol biosynthesis and cell proliferation through toll-like receptor 2 and toll-like receptor 4 pathways.[8] Consistently, stool collected from patients with CRC had more *F nucleatum* and *P anaerobius*, along with *Peptostreptococcus stomatis*, *Parvimonas micra*, *Solobacterium moorei*, and *Gemella morbillorum* that can form a co-occurring bacterial network in CRC.[12] Our results supported existence of a cancer-specific signature that harbored constituent microbial members that drove intestinal tumorigenesis. Nevertheless, in contrast to the dominant-pathogen model in infectious diseases, CRC appears to be influenced by keystone pathogens.[22] These keystone pathogens can co-opt with other species, remodel the microbiota, and alter the tumor milieu despite their relatively low abundance. Based on this model, it is important to consider effects of a polymicrobial consortium rather than an individual bacterium. This study provides unique data on the in vivo effects of a polymicrobial mixture from patients with CRC, and shows that the CRC microbiota is promoting carcinogenesis rather than protecting against it. Despite evolving changes with time, the microbiota of the recipient mice remained distinctively different between case-control groups, compatible with the presence of a cancer-specific signature in the CRC microbiota.

A previous well-conducted study with stool gavage from patients with CRC failed to recapitulate the human phenotype in germ-free mice.[23] The investigators used AOM to initiate tumor formation and dextran sulfate sodium (DSS) to inflict inflammation at 3 weeks after gavage of human stool. The tumor incidence in recipient mice was linked to the baseline microbial structure, but not the disease status of the donors. Nevertheless, although AOM induces cellular changes similar to human CRC in many aspects[24] and that the AOM/DSS model has been used extensively to model colitis-associated tumor, inflammation caused by DSS can alter the intestinal environment and microbiota.[25] This may have overwhelmed the effects of the transferred microbiota. By using the AOM-alone model, we avoided the undesirable influences from the chemically induced inflammation while keeping components that resemble human CRC, including early mutations in APC or beta-catenin signaling.[26] This also minimizes the intrinsic variability of the AOM/DSS model. Together with the germ-free model, we herein provide strong evidence for the tumorigenic effects of the CRC microbiota.

Our microarray data suggest that the CRC microbiota may evoke multiple inflammatory and oncogenic pathways in colorectal carcinogenesis. We observed significant increases in *Il17a, Il22*, and *Il23a*, implicating the Th17 cell response as a major pathway activated by the CRC microbiota.[5] Multiple studies have shown involvement of the Th17 pathway in colorectal tumorigenesis, as IL22 and IL23 both enhanced tumorigenesis in colitis-associated cancer models,[27,28] whereas blockade of IL17A inhibited tumor growth.[5,29] Our results highlight the importance of the Th17 pathway activated by microbial products. The up-regulation of *Cxcr1*, *Cxcr2*, and other membrane receptor genes suggested the importance of immune cell chemotaxis. This is consistent with previous literature showing the role of myeloid cells in modulating tumor microenvironment.[6] Furthermore, the microarray showed increased expressions of several cell-proliferation genes, including *Mki67*, which encodes for a proliferation marker, and *Mcm2*, *Aurka*, and *Cdc20*, which encode for proteins essential in regulating cell division. Minichromosome maintenance complex component 2 forms part of the replicative helicase that opens the replication fork during DNA replication. Aurora kinase A, the protein product of *Aurka*, is responsible for segregating centromeres during mitosis and translation of neural mRNA during meiosis. Cell-division cycle protein 20 interacts with cadherin-1 to regulate anaphase-promoting complex and cyclin-dependent kinases during cell cycle. Dysregulation of Aurora kinase A has been associated with cancers of the lung,[30] prostate,[31] and breast.[32]

We have performed oral gavage using human stool in this experiment. It should be noted, however, that the fecal microbiota is different from the mucosal microbiota, which may be more relevant to colorectal carcinogenesis.[33] Although some commensal bacteria live in the suspension in intestinal lumen,[34] some pro-tumorigenic bacteria may act through direct contact with epithelial cells, such as *F nucleatum*, which binds to adenocarcinoma cells to recruit proinflammatory myeloid cells,[6,35] and *P anaerobius*, which interacts with Toll-like receptors 2 and 4 on colonic epithelial cells.[8] On the other hand, a specific strain of *B fragilis* can secrete a metalloprotease toxin to mediate inflammation through a selective Th17 response.[5] Despite insufficient taxonomical resolution to the strain level, our

data showed increased *B fragilis* in the fecal microbiota of mice receiving CRC stool, associated with increased expressions of genes in the Th17 pathway. It is important that the different microbiota at the mucosae and in stool be considered, as the latter may not necessarily reflect the intestinal microenvironment directly pertaining to colorectal neoplasia.

In this study, we provide direct evidence of the protumorigenic roles of the CRC microbiota. These data extend our previous work to provide evidence for microbial dysbiosis in CRC, and suggest existence of a defined set of microbiota of which the composition is important. Our study is also distinct in taking a holism approach, given the observation of important bacterial networks in our previous association studies and evidence for the keystone pathogen hypothesis in CRC. Further studies will be required to disentangle how these keystone species interact with other members of the microbiota in colorectal carcinogenesis.

Supplementary Material

Note: To access the supplementary material accompanying this article, visit the online version of *Gastroenterology* at www.gastrojournal.org, and at https://doi.org/10.1053/j.gastro.2017.08.022.

References

1. Dove WF, Clipson L, Gould KA, et al. Intestinal neoplasia in the ApcMin mouse: independence from the microbial and natural killer (beige locus) status. Cancer Res 1997; 57:812–814.
2. Reddy BS, Narisawa T, Wright P, et al. Colon carcinogenesis with azoxymethane and dimethylhydrazine in germ-free rats. Cancer Res 1975;35:287–290.
3. Arthur JC, Perez-Chanona E, Muhlbauer M, et al. Intestinal inflammation targets cancer-inducing activity of the microbiota. Science 2012;338:120–123.
4. Cuevas-Ramos G, Petit CR, Marcq I, et al. *Escherichia coli* induces DNA damage in vivo and triggers genomic instability in mammalian cells. Proc Natl Acad Sci U S A 2010;107:11537–11542.
5. **Wu S, Rhee KJ**, Albesiano E, et al. A human colonic commensal promotes colon tumorigenesis via activation of T helper type 17 T cell responses. Nat Med 2009; 15:1016–10122.
6. Kostic AD, Chun E, Robertson L, et al. *Fusobacterium nucleatum* potentiates intestinal tumorigenesis and modulates the tumor-immune microenvironment. Cell Host Microbe 2013;14:207–215.
7. **Rubinstein MR, Wang X**, Liu W, et al. *Fusobacterium nucleatum* promotes colorectal carcinogenesis by modulating E-cadherin/beta-catenin signaling via its FadA adhesin. Cell Host Microbe 2013;14:195–206.
8. Tsoi H, Chu ES, Zhang X, et al. *Peptostreptococcus anaerobius* induces intracellular cholesterol biosynthesis in colon cells to induce proliferation and causes dysplasia in mice. Gastroenterology 2017;152:1419–1433.e5.
9. **Zeller G, Tap J, Voigt AY**, et al. Potential of fecal microbiota for early-stage detection of colorectal cancer. Mol Syst Biol 2014;10:766.
10. **Feng Q, Liang S, Jia H**, et al. Gut microbiome development along the colorectal adenoma-carcinoma sequence. Nat Commun 2015;6:6528.
11. **Nakatsu G, Li X, Zhou H**, et al. Gut mucosal microbiome across stages of colorectal carcinogenesis. Nat Commun 2015;6:8727.
12. **Yu J, Feng Q, Wong SH**, et al. Metagenomic analysis of faecal microbiome as a tool towards targeted non-invasive biomarkers for colorectal cancer. Gut 2017;66:70–78.
13. Schloss PD, Westcott SL, Ryabin T, et al. Introducing mothur: open-source, platform-independent, community-supported software for describing and comparing microbial communities. Appl Environ Microbiol 2009;75:7537–7541.
14. Needleman SB, Wunsch CD. A general method applicable to the search for similarities in the amino acid sequence of two proteins. J Mol Biol 1970;48:443–453.
15. **Quast C, Pruesse E, Yilmaz P**, et al. The SILVA ribosomal RNA gene database project: improved data processing and web-based tools. Nucleic Acids Res 2013; 41:D590–D596.
16. DeSantis TZ Jr, Hugenholtz P, Keller K, et al. NAST: a multiple sequence alignment server for comparative analysis of 16S rRNA genes. Nucleic Acids Res 2006; 34:W394–W399.
17. Edgar RC, Haas BJ, Clemente JC, et al. UCHIME improves sensitivity and speed of chimera detection. Bioinformatics 2011;27:2194–2200.
18. Cole JR, Wang Q, Fish JA, et al. Ribosomal Database Project: data and tools for high throughput rRNA analysis. Nucleic Acids Res 2014;42:D633–D642.
19. Westcott SL, Schloss PD. OptiClust, an Improved method for assigning amplicon-based sequence data to operational taxonomic units. mSphere 2017:2.
20. Segata N, Izard J, Waldron L, et al. Metagenomic biomarker discovery and explanation. Genome Biol 2011;12:R60.
21. Dembele D, Kastner P. Fold change rank ordering statistics: a new method for detecting differentially expressed genes. BMC Bioinformatics 2014;15:14.
22. Hajishengallis G, Darveau RP, Curtis MA. The keystone-pathogen hypothesis. Nat Rev Microbiol 2012;10: 717–725.
23. **Baxter NT, Zackular JP**, Chen GY, et al. Structure of the gut microbiome following colonization with human feces determines colonic tumor burden. Microbiome 2014;2:20.
24. Neufert C, Becker C, Neurath MF. An inducible mouse model of colon carcinogenesis for the analysis of sporadic and inflammation-driven tumor progression. Nat Protoc 2007;2:1998–2004.
25. Hakansson A, Tormo-Badia N, Baridi A, et al. Immunological alteration and changes of gut microbiota after dextran sulfate sodium (DSS) administration in mice. Clin Exp Med 2015;15:107–120.
26. De Robertis M, Massi E, Poeta ML, et al. The AOM/DSS murine model for the study of colon carcinogenesis:

From pathways to diagnosis and therapy studies. J Carcinog 2011;10:9.
27. Grivennikov SI, Wang K, Mucida D, et al. Adenoma-linked barrier defects and microbial products drive IL-23/IL-17-mediated tumour growth. Nature 2012; 491:254–258.
28. Huber S, Gagliani N, Zenewicz LA, et al. IL-22BP is regulated by the inflammasome and modulates tumorigenesis in the intestine. Nature 2012;491:259–263.
29. Chae WJ, Gibson TF, Zelterman D, et al. Ablation of IL-17A abrogates progression of spontaneous intestinal tumorigenesis. Proc Natl Acad Sci U S A 2010;107: 5540–5544.
30. Zhong N, Shi S, Wang H, et al. Silencing Aurora-A with siRNA inhibits cell proliferation in human lung adenocarcinoma cells. Int J Oncol 2016;49:1028–1038.
31. Monn MF, Cheng L. Emerging trends in the evaluation and management of small cell prostate cancer: a clinical and molecular perspective. Expert Rev Anticancer Ther 2016;16:1029–1037.
32. **Hou L, Chen M**, **Wang M**, et al. Systematic analyses of key genes and pathways in the development of invasive breast cancer. Gene 2016;593:1–12.
33. Sobhani I, Tap J, Roudot-Thoraval F, et al. Microbial dysbiosis in colorectal cancer (CRC) patients. PLoS One 2011;6:e16393.
34. van der Waaij LA, Harmsen HJ, Madjipour M, et al. Bacterial population analysis of human colon and terminal ileum biopsies with 16S rRNA-based fluorescent probes: commensal bacteria live in suspension and have no direct contact with epithelial cells. Inflamm Bowel Dis 2005;11:865–871.
35. **Abed J, Emgard JE**, Zamir G, et al. Fap2 mediates *Fusobacterium nucleatum* colorectal adenocarcinoma enrichment by binding to tumor-expressed Gal-GalNAc. Cell Host Microbe 2016;20:215–225.

Author names in bold designate shared co-first authorship.

Received February 2, 2017. Accepted August 9, 2017.

Reprint requests
Address requests for reprints to: Jun Yu, MD, PhD, Institute of Digestive Disease and Department of Medicine and Therapeutics, Prince of Wales Hospital, The Chinese University of Hong Kong, Shatin, NT, Hong Kong. e-mail: junyu@cuhk.edu.hk; fax: (852) 21445330; or Hong Wei, PhD, Department of Laboratory Animal Science, College of Basic Medical Sciences, Third Military Medical University, Chongqing, China. e-mail: weihong63528@163.com.

Conflicts of interest
The authors disclose no conflicts.

Funding
This project was supported by SHHO Foundation to research on microbiota in colorectal cancer, 973 Program China (2013CB531401), The National Key Technology R&D Program (2014BAI09B05), RGC-GRF Hong Kong (766613, 14106415, 14111216), 135 program project (2016YFC1303200), and Shenzhen Virtual University Park Support Scheme to CUHK-Shenzhen Research Institute. S.H.W. is supported by the Croucher Foundation. The funders have no role in the study design, collection, analysis, and interpretation of data.

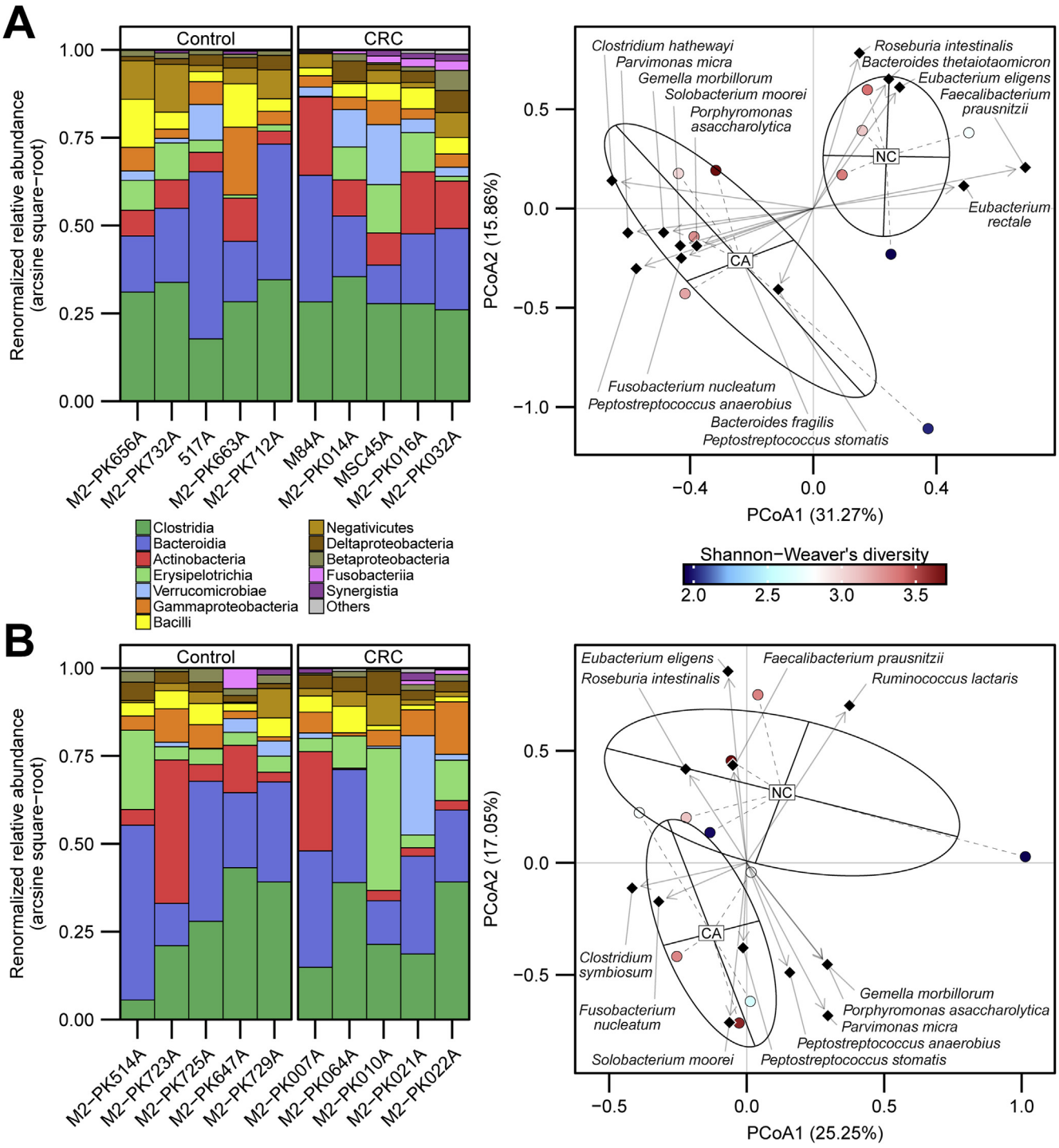

Supplementary Figure 1. Gut microbiota analysis of donor stools for murine stool gavage models. (*A*) Left-panel: hierarchical Ward D clustering of Canberra sample distance of relative bacterial class abundance in donor stools for AOM mice; data are rescaled after arcsine square-root transformation. Right-panel: Bray-Curtis distance-based PCoA biplot with biweight mid-correlations showing separation of donor stools for AOM mice (NC, healthy control, n = 5; CA, colorectal cancer, n = 5). (*B*) Left-panel: hierarchical Ward D clustering of Canberra sample distance of relative bacterial class abundance in donor stools for GF mice; data are rescaled after arcsine square-root transformation. Right-panel: Bray-Curtis distance-based PCoA biplot with biweight mid-correlations showing separation of donor stools for GF mice (NC, healthy control, n = 5; CA, colorectal cancer, n = 5).

Supplementary Table 1. Details of Colonic Polyps in the 3 Groups of Mice in the AOM Model

Group	CRC-A	HC-A	NC-A	HC-A + NC-A
Treatment	Gavage with CRC stool	Gavage with healthy control stool	No stool gavage control (given PBS)	Combined controls
Total no. mice	11	12	10	22
Mice with polyp, n (%)	7 (63.6)	2 (16.7)	1 (10.0)	3 (13.6)
Total no. polyps (average per mouse)	16 (1.45)	5 (0.42)	1 (0.1)	6 (0.27)
Poly size, mm, mean ± SD	1.95 ± 0.53	1.80 ± 0.22	1.70 ± 0.00	1.78 ± 0.20
High-grade dysplasia, n (%)	3 (27.3)	0 (0)	0 (0)	0 (0)
Any dysplasia, n (%)	6 (54.5)	3 (25.0)	2 (20.0)	5 (22.7)
Inflammation, n (%)	9 (81.8)	4 (33.3)	4 (40.0)	8 (36.4)
Composite histology score, mean ± SD	4.45 ± 1.81	2.92 ± 1.24	2.70 ± 1.77	2.82 ± 1.47

Supplementary Table 2. Clinical Characteristics of the Human Donors for Stool Gavage to Mice in the AOM Model

	CRC cases					Healthy controls				
Age	89	67	74	54	69	51	62	64	69	65
Sex	Female	Female	Male	Female	Female	Male	Female	Female	Male	Female
Body mass index	23.7	24.7	26.7	25.6	28.3	21.9	21.1	21.3	23.8	20.0
Smoker	No	No	Ex-smoker	Yes	Yes	Yes	No	No	No	No
Diabetes mellitus	Yes	No	Yes	No	No	Yes	No	No	Yes	Yes
CRC stage	2	3	3	4	4	N/A	N/A	N/A	N/A	N/A
TNM stage	T3N0M0	T3N1M0	T4N2M0	T4N1M1	T4N2M1	N/A	N/A	N/A	N/A	N/A
Site of tumor	Cecum	Sigmoid	Descending	Recto-sigmoid	Rectum	N/A	N/A	N/A	N/A	N/A

N/A, not applicable.

Supplementary Table 3. Clinical Characteristics of the Human Donors for Stool Gavage to Mice in the Germ-Free Model

	CRC cases					Healthy controls				
Age	64	56	67	57	51	64	64	58	70	62
Sex	Female	Male	Male	Male	Male	Female	Female	Male	Female	Male
Body mass index	22.6	22.2	26.3	22.2	23.5	29.1	25.6	23.1	23.2	26.9
Smoker	No	Yes	Yes	Yes	No	Yes	No	No	Yes	Yes
Diabetes mellitus	No	No	No	Yes	Yes	No	Yes	Yes	No	No
CRC stage	3	3	2	2	3	N/A	N/A	N/A	N/A	N/A
TNM stage	T3N1M0	T3N1M0	T3N0M0	T4N0M0	T3N0M0	N/A	N/A	N/A	N/A	N/A
Site of tumor	Rectosigmoid	Rectum	Descending	Sigmoid	Rectum	N/A	N/A	N/A	N/A	N/A

N/A, not applicable.

Supplementary Table 4. Relative Abundance of Selected Bacteria With Putative Pro-tumorigenic Role in CRC

Sample	Group	*Escherichia coli*, %	*Bacteroides fragilis*, %	*Fusobacterium nucleatum*, %	*Parvimonas micra*, %	*Solobacterium moorei*, %	*Peptostreptococcus anaerobius*, %	*Peptostreptococcus stomatis*, %	*Gamella morbillorum*, %
M2-PK514A	HC-A	0.243	5.261	0	0	0.006	0	0	0
M2-PK647A	HC-A	1.058	0.414	0	0	0	0	0	0
M2-PK723A	HC-A	62.476	0.113	0	0	0	0	0	0
M2-PK725A	HC-A	0.271	0.585	0	0	0	0	0	0
M2-PK729A	HC-A	0.343	0	0	0	0	0	0	0
M2-PK007A	CRC-A	12.187	0.015	0	0	0	0	0.008	0.206
M2-PK010A	CRC-A	0.317	0.152	0	0.324	0.006	0	0.512	1.138
M2-PK021A	CRC-A	0.295	1.132	0.034	0.051	0.007	0.069	0.338	0.130
M2-PK022A	CRC-A	0.047	3.987	0.026	0.228	0.002	1.677	0.085	0
M2-PK064A	CRC-A	0	0	0	0	0.002	0	0	0
517A	HC-G	1.299	0.009	0	0	0	0	0	0
M2-PK656A	HC-G	0.160	0.021	0	0	0.001	0	0	0
M2-PK663A	HC-G	18.502	0	0	0	0	0	0	0
M2-PK712A	HC-G	0.007	0	0	0	0	0	0	0
M2-PK732A	HC-G	0.097	0	0	0	0	0	0	0
M2-PK014A	CRC-G	0.724	0.882	0.044	0.132	0.159	1.741	2.688	0
M2-PK016A	CRC-G	0.317	4.675	0.332	1.033	1.769	0.001	1.201	2.005
M2-PK032A	CRC-G	0.890	0.037	0.017	0.789	0.008	0.984	1.237	1.064
M84A	CRC-G	0.327	0.015	0.003	0	0.003	0	0.003	0.001
MSC45A	CRC-G	3.283	0	0	0.146	0.085	0.284	0.522	0.013

Supplementary Table 5. Comparisons of Community Richness and Diversity Indexes in Mice Transplanted With CRC or Healthy Stools

Index	Group	Comparison	*Z*-statistic	*P*
Observed community richness (sobs)	AOM mice	CRC-A vs HC-A	2.585	.010
Chao1 community richness	AOM mice	CRC-A vs HC-A	3.385	7.1×10^{-4}
Fisher's alpha diversity	AOM mice	CRC-A vs HC-A	2.585	.010
Shannon-Weaver's diversity	AOM mice	CRC-A vs HC-A	1.169	.242
Observed community richness (sobs)	Germ-free	CRC-G vs HC-G (8 wk)	2.803	.005
Chao1 community richness	Germ-free	CRC-G vs HC-G (8 wk)	0.550	.624
Fisher's alpha diversity	Germ-free	CRC-G vs HC-G (8 wk)	2.803	.005
Shannon-Weaver's diversity	Germ-free	CRC-G vs HC-G (8 wk)	4.273	1.93×10^{-5}

Supplementary Table 6. List of Genes Showing Up-regulation for More Than Twofold, in AOM and Germ-Free Mice Gavaged With Stools From CRC Cases Vs Healthy Controls: Expression Levels Were Compared Using the Mouse Inflammatory Response and Autoimmunity PCR Array

Gene name	Full name	Fold change (AOM)	Fold change (germ-free)
Cxcr2	Chemokine (C-X-C motif) receptor 2	15.065	38.519
Cxcr1	Chemokine (C-X-C motif) receptor 1	16.9047	30.2214
Il17a	Interleukin 17A	46.9383	8.2107
Il5	Interleukin 5	50.2798	3.5004
Il22	Interleukin 22	19.6473	6.2658
Il9	Interleukin 9	12.7552	4.9847
Tnfsf14	Tumor necrosis factor (ligand) superfamily, member 14	12.7571	4.3394
Cxcl5	Chemokine (C-X-C motif) ligand 5	16.7085	3.0898
Cxcl9	Chemokine (C-X-C motif) ligand 9	9.0641	5.6081
Ccl1	Chemokine (C-C motif) ligand 1	10.8771	4.5552
Il10	Interleukin 10	12.1244	4.0488
Cxcl11	Chemokine (C-X-C motif) ligand 11	16.7038	2.9029
Sele	Selectin, endothelial cell	22.7855	2.0669
Kng1	Kininogen 1	8.1982	5.4926
Il23r	Interleukin 23 receptor	9.8361	3.0262
Ccr4	Chemokine (C-C motif) receptor 4	8.8671	2.4242
Cxcl10	Chemokine (C-X-C motif) ligand 10	9.0156	2.0813
Cxcl1	Chemokine (C-X-C motif) ligand 1	6.3651	2.5097
Ifng	Interferon gamma	5.3737	2.9029
Tlr6	Toll-like receptor 6	5.7979	2.6712
Ccl19	Chemokine (C-C motif) ligand 19	6.3207	2.2153
Il23a	Interleukin 23, alpha subunit p19	4.5351	2.8629
Ccl12	Chemokine (C-C motif) ligand 12	3.0661	4.0488
Ccl17	Chemokine (C-C motif) ligand 17	5.6877	2.1104
Ccl7	Chemokine (C-C motif) ligand 7	2.1361	5.3796
Ccl20	Chemokine (C-C motif) ligand 20	2.7769	3.8304
Ccl4	Chemokine (C-C motif) ligand 4	4.7713	2.0958
Ccl3	Chemokine (C-C motif) ligand 3	3.6683	2.2462
Ccl2	Chemokine (C-C motif) ligand 2	3.037	2.6898
Lta	Lymphotoxin A	2.769	2.5624
Ccl22	Chemokine (C-C motif) ligand 22	2.6352	2.0669
Ccl8	Chemokine (C-C motif) ligand 8	2.5934	2.0669
Il1rn	Chemokine (C-X-C motif) receptor 2	15.065	38.519

Supplementary Table 7. List of Genes Showing Up-regulation for More Than Twofold, in AOM and Germ-Free Mice Gavaged With Stools From CRC Cases Vs Healthy Controls: Expression Levels Were Compared Using the Mouse Cancer Pathway Finder PCR Array

Gene name	Full name	Fold change (AOM)	Fold change (germ-free)
Mcm2	Minichromosome maintenance deficient 2 mitotin	3.9085	313.6109
Serpinb2	Serine (or cysteine) peptidase inhibitor, clade B, member 2	8.5695	98.4522
Gsc	Goosecoid homeobox	17.3126	23.0789
Fasl	Fas ligand (TNF superfamily, member 6)	10.1022	26.8009
Snai1	Snail homolog 1 (*Drosophila*)	7.4823	28.6599
Krt14	Keratin 14	11.1049	15.0496
Ercc3	Excision repair cross-complementing rodent repair deficiency, complementation group 3	3.6177	42.3119
G6pdx	Glucose-6-phosphate dehydrogenase X-linked	4.157	25.237
Foxc2	Forkhead box C2	6.3925	16.2626
E2f4	E2F transcription factor 4	12.4565	8.0886
Vegfc	Vascular endothelial growth factor C	7.5196	10.8943
Ccl2	Chemokine (C-C motif) ligand 2	5.4746	11.4127
Gadd45g	Growth arrest and DNA-damage-inducible 45 gamma	5.7263	8.3315
Lpl	Lipoprotein lipase	3.245	10.7996
Snai3	Snail homolog 3 (*Drosophila*)	2.885	11.9692
Angpt1	Angiopoietin 1	3.216	10.1281
Fgf2	Fibroblast growth factor 2	6.8317	4.7532
Flt1	FMS-like tyrosine kinase 1	7.9856	4.0072
Sox10	SRY-box containing gene 10	7.4456	3.4741
Mki67	Antigen identified by monoclonal antibody Ki-67	9.3579	2.6748
Cdc20	Cell division cycle 20 homolog (*Saccharomyces cerevisiae*)	7.4953	3.3302
Pgf	Placental growth factor	3.5493	6.995
Pinx1	PIN2/TERF1 interacting, telomerase inhibitor 1	9.3754	2.6185
Tek	Endothelial-specific receptor tyrosine kinase	4.1052	5.9788
Ercc5	Excision repair cross-complementing rodent repair deficiency, complementation group 5	7.0219	3.2438
Bmi1	Bmi1 polycomb ring finger oncogene	8.6985	2.477
Kdr	Kinase insert domain protein receptor	5.091	4.029
Xiap	X-linked inhibitor of apoptosis	7.6499	2.6515
Cdh2	Cadherin 2	3.9141	5.032
Cflar	CASP8 and FADD-like apoptosis regulator	4.1179	3.4828
Ccnd2	Cyclin D2	5.0881	2.1563
Gpd2	Glycerol phosphate dehydrogenase 2, mitochondrial	4.3562	2.3986
Aurka	Aurora kinase A	3.5151	2.7733
Birc3	Baculoviral IAP repeat-containing 3	4.0484	2.1275
Tbx2	T-box 2	3.0581	2.2202
Serpinf1	Serine (or cysteine) peptidase inhibitor, clade F, member 1	2.1311	2.7509
Sirt1	Sirtuin 1 (silent mating type information regulation 2, homolog) 1	2.0648	2.0387